Availability Study of FSO Systems in Europe

Zdenek Kolka, Viera Biolkova, Dalibor Biolek

Abstract— The paper presents a study of the availability of Free Space Optical communication links based on data obtained by long-term measurement. Visibility records collected from 210 European airports were analyzed to obtain a realistic estimation of the availability of wireless optical technology. Commercially available optical links operate mostly in the 850nm waveband, where the influence of the atmosphere on the optical beam and on the visible light is similar. The model used characterizes both the statistical properties of fade depths and the statistical properties of individual fade durations. Results are presented for selected European cities.

Keywords— Free space optical link, scattering, atmospheric channel, availability.

I. INTRODUCTION

RECENT development of municipal communication infrastructure is characterized by progressive adoption of optical technology. Fiber-to-the-Home (FTTH) networks based on the Passive Optical Network (PON) technology bring multi-megabit transmission rates to end subscribers [1]. The dominantly fiber infrastructure can be completed with the broadband Free Space Optical (FSO) technology.

The main attraction of FSO technology is the bandwidth comparable to optical fibers since both systems operate on the same physical principle. The wireless aspect of FSO can be a crucial advantage in cities where the laying of optical cables is impossible or expensive. In addition, the optical band used for communication is still license-free.

The available optical band for atmospheric wireless links ranges theoretically from 0.7 μm to 10 μm [2]. Fog is the most important environmental factor causing almost *wavelength-independent* attenuation, which might reach 400dB/km [3], [4]. Therefore it is advantageous to use communication windows that are shared with optical fibers (i.e. 850nm and 1550nm) as the manufacturing cost of FSO units can be kept at a reasonable level using components already developed for fiber systems.

The attenuation of atmospheric channel is time- and space-varying due to:

- Scattering on hydrometeors during fog, snow, and heavy rain. Attenuation caused by thick fog can reach 400dB/km [3]. If this slowly-varying attenuation is greater than the link margin, the communication is completely cut-off for hours or even days.
- Misalignment of relatively narrow beams caused by buildings swaying due to thermal gradient, wind and vibration [5].
- Atmospheric turbulence causing received-power fluctuations on the millisecond time scale. The effect of turbulence is often modeled on a sufficiently long time scale by introducing a power penalty [6].

The overall availability of FSO links is influenced by the occurrence of fog events, which depends, of course, on geographic location. Increasing the availability by means of increasing the output power is very expensive and also has physical and safety limits [4].

A further increase in link availability can be achieved by combining the FSO link with a radio-frequency (RF) link. The main environmental factor influencing RF links is the scattering and absorption on rain droplets whereas attenuation due to fog is not significant [7], [14], [15].

The deployment of FSO or hybrid technology depends on a realistic estimation of attainable parameters. Several studies have been published on availability performance [11]-[14]. But most of them are based on observations carried out on few sites. This paper presents a comprehensive availability study for European climatic conditions. The study is based on long-term observation of atmospheric attenuation done at European airports. Section 2 of the paper presents a model of the FSO atmospheric channel used for the analysis, and Section 3 provides statistical characterization of availability for major European cities.

II. MODEL OF ATMOSPHERIC CHANNEL

A. Attenuation in Optical Band

The mean optical power $P_{m,RXA}$ on the receiving aperture of an FSO terminal is given by the power budget equation (in decibels) [8]

$$P_{m,RXA} = P_{m,TXA} - \alpha_{sys} - \alpha_{atm} \ , \tag{1}$$

where $P_{m,TXA}$ is the mean optical power on the transmitting aperture. The system attenuation α_{sys} includes all constant losses and gains that depend only on transceiver design and path length L_{12}

This work was supported by the Czech Science Foundation under projects No. 102/08/0851, No. 102/09/0550, the Czech Ministry of Education under research project No. MSM0021630513. The research leading to these results has received funding from the European Community's Seventh Framework Programme (FP7/2007-2013) under *grant agreement* No. 230126.

Z. Kolka is with the Department of Radio Electronics, Brno University of Technology, Brno, Czech Republic (e-mail: kolka@feec.vutbr.cz).

V. Biolkova is with the Department of Radio Electronics, Brno University of Technology, Brno, Czech Republic (e-mail: biolkova@feec.vutbr.cz).

D. Biolek is with the Department of Microelectronics, Brno University of Technology, Brno, Czech Republic (e-mail: biolek@feec.vutbr.cz).

$$\alpha_{sys} = 20\log\frac{L_{12}\varphi_T}{D_{RXA}} - \gamma_{add} \quad \text{for } L_{12}\varphi_t >> D_{RXA} \ , \tag{2}$$

where D_{RXA} is the diameter of receiving aperture, and φ_T is the full angle of beam divergence (for a drop to level $1/e^2$). For the Gaussian beam the additional gain stemming from the definition of φ_T is $\gamma_{add} = 3.7$ dB. Attenuation α_{atm} represents all random losses caused by atmospheric phenomena.

Link margin M is the difference between the mean received optical power without atmospheric effects and the receiver sensitivity threshold $P_{0,RXA}$ defined for a chosen BER performance, i.e.

$$M = P_{m,TXA} - \alpha_{sys} - P_{0,RXA} \ . \tag{3}$$

The upper bound for M is determined by the dynamical range of receiver and the Automatic Transmit Power Control (ATPC), if available.

The atmospheric attenuation can be expressed as a sum of absorption on atmospheric gases α_{ab}, scattering on hydrometeors α_{sc} and power penalty of turbulence α_{turb}

$$\alpha_{atm} = (\alpha_{1,sc} + \alpha_{1,ab})L_{12} + \alpha_{turb}(L_{12}) \ , \tag{4}$$

where $\alpha_{1,sc}$ and $\alpha_{1,ab}$ are the specific attenuation coefficients.

Theoretically, the power penalty of atmospheric turbulence could be expressed exactly if the probability density function of received power was known. In practice, α_{turb} can be estimated from the model of atmospheric turbulence with weather-dependent parameters and size of the receiving aperture [6]. A typical value is 4 dB for 1km link under moderate atmospheric turbulence [9].

The atmospheric attenuation due to molecular absorption is negligible for both 850 nm and 1550 nm bands.

The scattering attenuation, which is 0.5dB/km for the standard *clear* atmosphere, increases substantially during fog, snowfall and rain. The predominant process for light attenuation by fog is the Mie scattering [3]. Fog density is measured indirectly as the Meteorological Optical Range (MOR) or simply visibility range V_M, which is given by the Koschmieder law as

$$V_M = \frac{10\log_{10}(1/\eta)}{\alpha_{1,\lambda=550nm}} \ , \tag{5}$$

where η is 0.05 according to meteorological standards [10]. The attenuation is measured at 550nm with a spectral width of 250nm. The relation between $\alpha_{1,sc}$ and the visibility range V_M for other wavelengths has been discussed in many publications [11], [12] as it depends on fog density and particle size distribution. Empirical formulae were proposed by Kruse [13], Kim [11], and Al Naboulsi [12], Fig. 1. The relation between $\alpha_{1,sc}$ and V_M exhibits uncertainty of the order of ±20dB/km for $V_M \approx 100$m for practical observations [3].

Kim's formula [11] was used in this study since practical observations confirm the wavelength-independence of attenuation [14].

$$\alpha_{1,part} = \frac{13}{V_M}\left(\frac{\lambda}{550}\right)^{-q} \ [\text{dB/km}] \ , \tag{6}$$

where V_M is the meteorological visibility in km for $\eta = 0.05$, λ is the wavelength in nm, and q depends on V_M:

$q =$ 1.6 for $V_M > 50$ km;
1.3 for 6 km $< V_M \le 50$ km;
$0.16\ V_M + 0.34$ for 1 km $< V_M \le 6$ km;
$V_M - 0.5$ for 0.5 km $< V_M \le 1$ km;
0 for $V_M \le 0.5$ km.

Attenuation due to snow and rain can be considered negligible in comparison with fog [15].

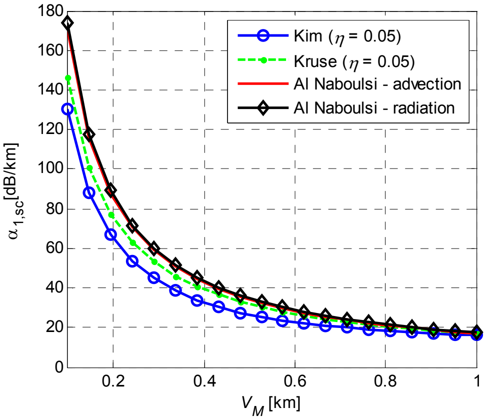

Fig. 1 Comparison of different formulae for $\alpha_{1,sc}$ for $\lambda = 850$nm

B. Statistical Model of Availability

Figure 2 shows the time behavior of received optical power at receiving aperture [8]. A fade event occurs when the total atmospheric attenuation exceeds the link margin M, i.e. when BER of the link exceeds a chosen level.

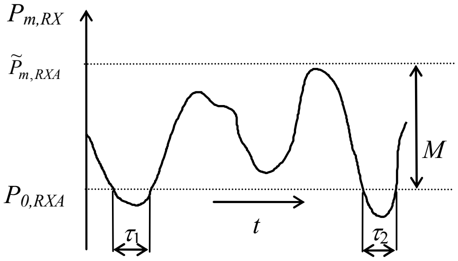

Fig. 2 Fade events on FSO link

Regarding the atmospheric attenuation α_{atm} as a random variable, the probability of link unavailability P_{un} can be expressed as

$$P_{un} = P(\alpha_{1,atm} \ge M_1) = E_\alpha(M_1) \ , \tag{7}$$

where M_1 is the specific link margin $M_1 = M / L_{12}$, and E_α is the cumulative exceedance probability of atmospheric attenuation.

If a fixed value of normalized link margin M_1 is considered, the increase of atmospheric attenuation causes fade events. Their durations form a random time series $\{\tau_i\}$, which can be characterized by the conditional exceedance probability

$$P(\tau \ge \tau^* \mid \alpha_{1,atm} \ge M_1) = E_{\tau|\alpha}(\tau^* \mid M_1) \ , \tag{8}$$

i.e. the probability that the fade duration is longer than τ^* in the case of a fade event deeper than M_1. $E_{\tau|\alpha}$ can be estimated from

$$E_{\tau|\alpha}(\tau^*|M_1) \approx \frac{n_{\tau_i \ge \tau^*}}{N} \ , \qquad (9)$$

where $n_{\tau_i \ge \tau^*}$ is the number of fade events longer than τ^*, and N is the total number of fade events during a sufficiently long period. Typically, the fade is deep. Thus $E_{\tau|\alpha}$ does not change dramatically with M_1.

III. AVAILABILITY OF FSO SYSTEMS IN EUROPE

The analysis is based on visibility observations carried out at airports. Records for 210 airports in Italy, France, and Germany for the years 2002 to 2005 with the sampling period ranging from 15 minutes to 1 hour were processed. Therefore the statistics cover only long-term outages of FSO links. The power penalty of scintillation was neglected in the analysis as the effect of atmospheric turbulence decreases during fog events.

All calculations were done for the 850nm optical band. The visibility resolution was 100m, which gives the largest recorded attenuation of about 130dB/km. Certain preprocessing was necessary since some records were incomplete or contained errors.

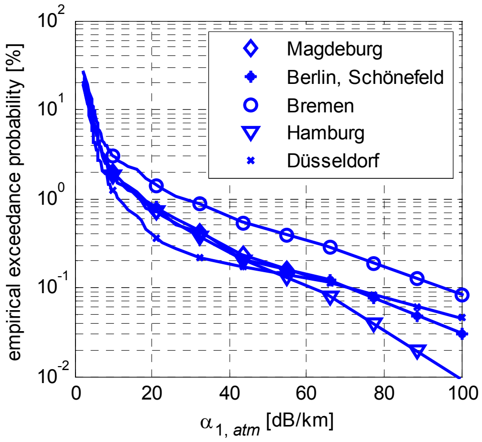

Fig. 3 Empirical E_α (unavailability) for selected sites in Germany.

TABLE I

LINK UNAVAILABILITYI IN % FOR SELECTED SITES IN GERMANY

Site	40dB/km	60dB/km	80dB/km	100dB/km
Dresden	0.31	0.22	0.11	0.051
Cologne	0.14	0.090	0.051	0.027
Nurnberg	0.15	0.072	0.026	0.0082
Leipzig	0.38	0.20	0.12	0.079
Hannover	0.44	0.26	0.16	0.10
Hamburg	0.18	0.033	0.014	0.0087
Dortmund	0.27	0.17	0.058	0.015
Bayreuth	1.24	0.67	0.31	0.14

Figures 3, 4, and 5 show empirical exceedance probabilities E_α for several cities in Europe. The curves for all the sites exhibit an evident knee below 20 dB/km. The exceedance probability above the knee is roughly linear in the semilogarithmic coordinates, which corresponds to an exponential-tail distribution. Tables I, II, and III show unavailability percentages for other sites for different values of normalized link margin M_1.

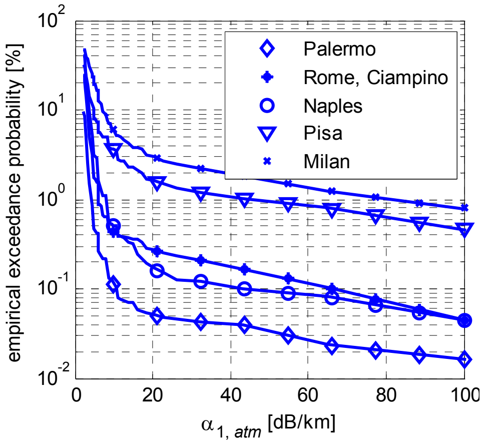

Fig. 4 Empirical E_α (unavailability) for selected sites in Italy.

TABLE II

LINK UNAVAILABILITYI IN % FOR SELECTED SITES IN ITALY

Site	40dB/km	60dB/km	80dB/km	100dB/km
Catania	0.043	0.028	0.020	0.014
Bergamo	0.95	0.62	0.40	0.26
Torino	1.05	0.77	0.52	0.33
Parma	0.82	0.46	0.28	0.17
Bologna	1.70	1.16	0.82	0.59
Verona	1.76	1.45	1.08	0.77
Firenze	0.66	0.44	0.29	0.19
Trieste	0.31	0.17	0.093	0.051

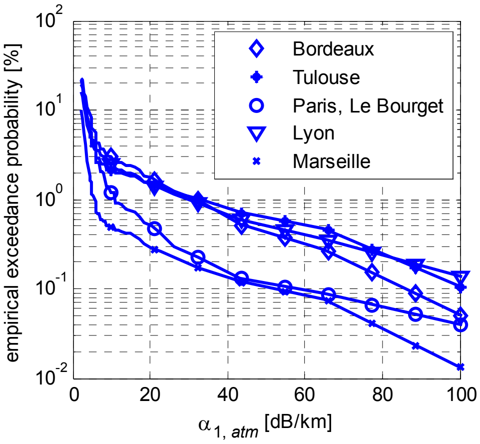

Fig. 5 Empirical E_α (unavailability) for selected sites in France.

TABLE III

LINK UNAVAILABILITYI IN % FOR SELECTED SITES IN FRANCE

Site	40dB/km	60dB/km	80dB/km	100dB/km
Grenoble	0.23	0.12	0.056	0.024
Vichy	0.78	0.48	0.30	0.19
Montpellier	0.19	0.098	0.057	0.034
Avignon	0.50	0.39	0.25	0.15
Orléans	1.02	0.58	0.24	0.090
Lille	1.30	0.87	0.56	0.35
Cherbourg	1.26	1.01	0.72	0.48
Strasbourg	0.96	0.53	0.29	0.15

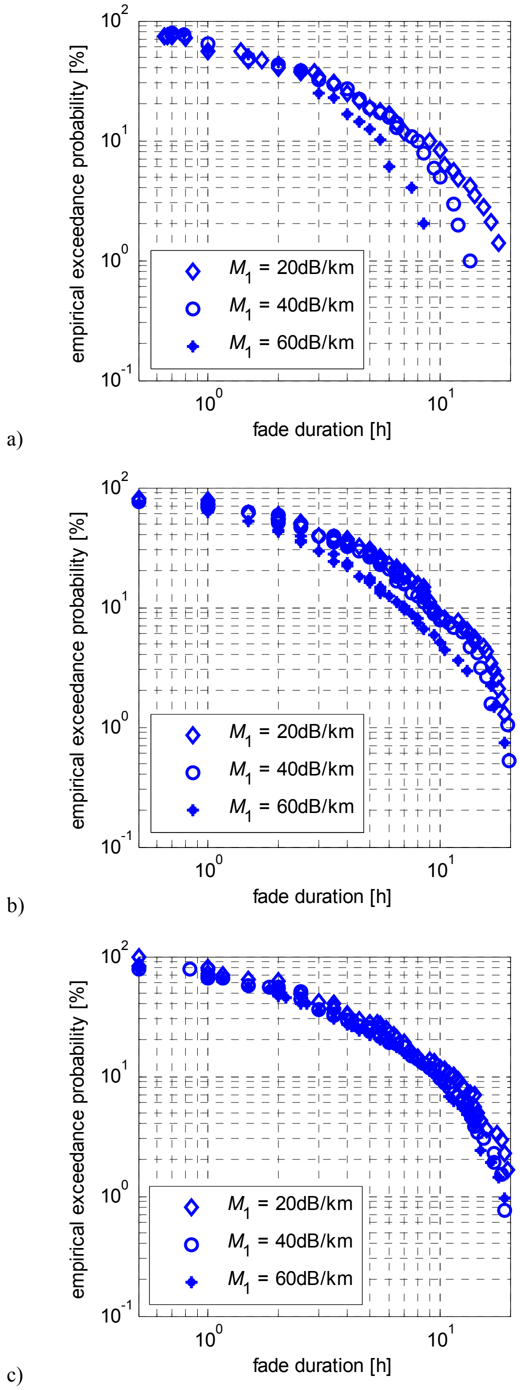

Fig. 6 Cumulative conditional exceedance probability of fade durations for different values of M_1; a) Lyon, b) Milan, c) Verona

Figure 6 shows the cumulative conditional exceedance probability of fade durations for selected sites. As can be seen, there is little dependence on the normalized link margin chosen, i.e. the fog events are usually deep. The typical fade length is in hours.

It conforms to figures 3 to 5 with the slope above 20dB/km decreasing very slowly. In order to increase the availability by one decade it is necessary to increase the link margin by 60 to 80dB, i.e. to increase the equivalent transmitted power by 6 to 8 orders of magnitude. This would require a prohibitively expensive design of FSO terminals.

IV. CONCLUSION

The paper presents realistic results for estimating FSO performance in Europe, based on long-term meteorological visibility observations. The simulated unavailability of FSO links ranges from 1% to 0.05% depending on the normalized link margin and geographical location.

As the typical link margin is 20dB, unavailability below 0.1% can be achieved in some locations for FSO path lengths of 250m, i.e. for a normalized link margin of 80dB/km.

A further increase of availability for moderately long links is prohibitively expensive. A feasible solution is represented by hybrid FSO/RF links.

REFERENCES

[1] S. Wright, H. Fahmy, and A. J. Vernon, “Deployment Challenges for Access/Metro Optical Networks and Services,” *IEEE J. Lightwave Techn.*, vol. 22, Nov. 2004, pp. 2606-2616.
[2] J. Schuster, H. Willebrand, S. Bloom, and E. Korevaar, “Understanding the performance of Free Space Optics,” *Journal of Optical Networking*, vol. 2, no. 6, 2003, pp .178-200.
[3] M. Gebhart, et al. “Measurement of Light Attenuation in Dense Fog Conditions for FSO Applications,” in *Proc. of SPIE*, vol. 5891, 2005, 58910K
[4] I. Kim, and E. Korevaar, “Availability of free-space optics (FSO) and hybrid FSO/RF systems,” in *Proc.of SPIE*, vol. 4530, 2003, pp. 84-95.
[5] S. Arnon, “Optimization of optical wireless communication systems,” *IEEE Trans. Wireless Comm.*, vol. 2, July 2003, pp. 626-629.
[6] D. Giggenbach, and H. Henniger, “Fading-loss assessment in atmospheric freespace optical communication links with on-off keying,”. *Optical Engineering*, vol. 47, April 2008, pp. 046001-1 - 046001-6.
[7] L. E. Allnut, *Satellite-to-ground radiowave propagation: Theory, practice and system impact at frequencies above 1GHz*. London: IEE, 1989.
[8] S. G. Lambert, W. L. Casey, *Communication in Space*, London: Artech House, 1995.
[9] Rec. ITU-R P.1814 “Prediction methods required for the design of terrestrial free-space optical links”, ITU, Geneva, Switzerland, Sept. 2008.
[10] Guide to Meteorological Instruments and Methods of Observation. World Meteorological Organization, Geneva, Switzerland, 2006.
[11] I. Kim, B. Mc Arthur, and E. Korevaar, “Comparison of laser beam propagation at 785 nm and 1550 nm in fog and haze for optical wireless communications,” in *Proc. of SPIE*, vol. 4214, 2001, pp. 26-37.
[12] M. Al Naboulsi, H. Sizun, and F. de Fornel, “Fog attenuation prediction for optical and infrared waves,” *Optical Engineering*, vol. 43, 2004, pp. 319-329.
[13] P. W. Kruse, L. D. Mc Glauchlin, and R. B. Mc Quistan, *Elements of Infrared Technology*. New York: Wiley, 1962.
[14] F. Nadeem, V. Kvicera, M. S. Awan, E. Leitgeb, S. S. Muhammad, G. Kandus, “Weather Effects on Hybrid FSO/RF Communication Link,” *IEEE J. on Selected Areas in Communications*, Vol. 27, No. 9, Dec. 2009.
[15] O. Wilfert, V. Kvicera, Z. Kolka, M. Grabner, O. Fiser, “Propagation study of 850nm/58 GHz hybrid municipal system,” in *Proc. of SPIE*, vol. 7814, 2010, DOI: 10.1117/12.860508.